# The Fe-V (Iron-Vanadium) System

55.847 50.9415

By J. F. Smith
Iowa State University

## Phase Relationships

**General Features.** The Fe-V system is a relatively simple system with an azeotropic minimum in its melting behavior, continuous solid solution at elevated temperatures, a closed $\gamma$ loop on the Fe-rich side, and an intermediate phase that forms congruently from the high-temperature solid solution near equiatomic stoichiometry. The assessed phase diagram is shown in Fig. 1. This diagram is a composite of available information. The solidus and liquidus are a combination of the calculated results of Hack *et al.* [79Hac] and of Andersson [83And]. The boundaries associated with the $\gamma$ loop are based on the experimental work of Fischer *et al.* [70Fis] and of Kirchner [70Kir] and have been corroborated by the calculations of Andersson [83And]. The boundaries associated with the $\sigma$ phase are taken from the work of Inden and Büth [83But]. The temperatures for the Fe transformations are taken from the review of Swartzendruber [82Swa], and the melting temperature of V is taken from the review of Smith [81Smi].

The melting minimum was first reported by Vogel and Tammann in 1908 [08Vog], the closed $\gamma$ loop was first reported by Maurer in 1925 [25Mau], and the continuous solid solution at elevated temperatures with congruent transformation to a lower temperature intermediate phase was first reported by Wever and Jellinghaus in 1930 [30Wev]. This early work, together with subsequent investigations, was considered in the review of the system that was included in the recently published survey of the binary Fe systems by Ortrud Kubaschewski [82Kub]. The present work supplements this review primarily in the incorporation of the quite recent results of Andersson [83And] and of Inden and Büth [83But] and in the addition of data concerning magnetic, crystallographic, and thermodynamic aspects of the system.

**Liquidus and Solidus.** It is well established that there is an azeotropic melting minimum in the Fe-V system, and there is remarkably good agreement with regard to the temperature and composition associated with this azeotropic minimum. Vogel and Tammann [08Vog] initially reported the minimum at 34 at.% V and 1435 °C, Wever and Jellinghaus [30Wev] at 33 at.% V and 1468 °C, Hellawell and Hume-Rothery [57Hel] at 30.5 at.% V and 1473.5 °C, Furukawa and Kato [75Fur] at 32 at.% V and 1470 °C, and Oswald Kubaschewski *et al.* [77Kub] at 35 at.% V and 1468 °C. Because the minimum tends to be relatively flat, the spread between 30.5 and 35 at.% V is not significant, and the calculated value of 31 at.% V can be considered as quite satisfactory agreement. Furthermore, if one discounts the early value of 1435 °C from Vogel and Tammann [08Vog] because of purity, the calculated temperature of 1468 °C is in very good accord with the experimental values. Therefore, the experimental liquidus and solidus points of Hellawell and Hume-Rothery [57Hel] in

**Fig. 1 Assessed Fe-V Phase Diagram**

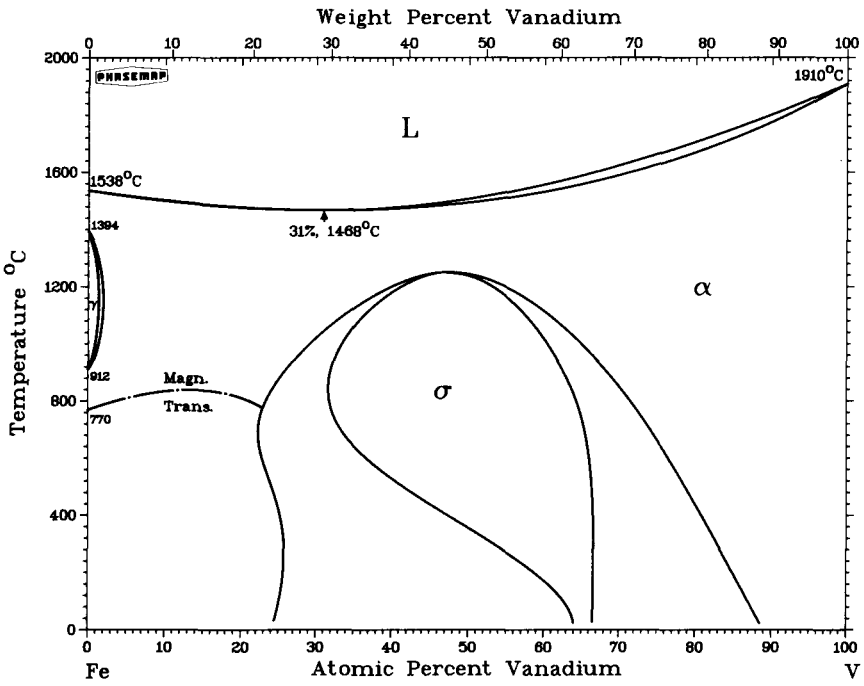


J. F. Smith, 1984.

**Fig. 2 Effect of Pressure on the γ Loop in the Fe-V System**

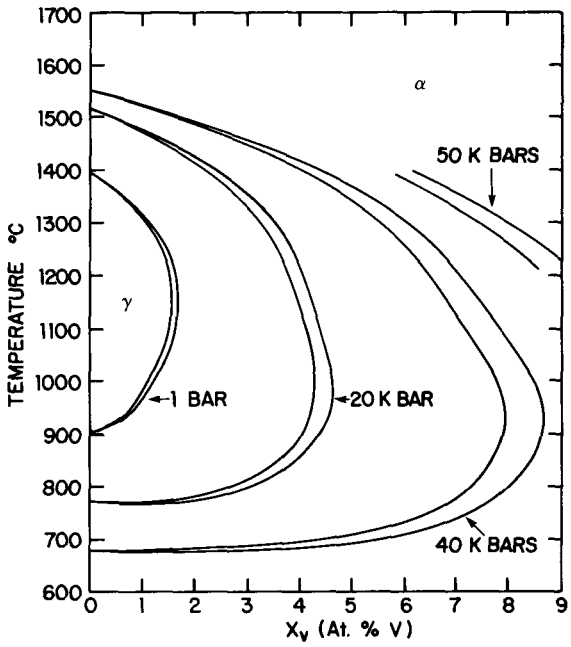


As determined by Hanneman *et al.* [65Han]. Their boundaries for loop at 1 bar ambient pressure vary slightly from the accepted values in Fig. 1 and 5. J. F. Smith, 1984.

the composition range 0 to 40 at.% V and of Furukawa and Kato [75Fur] in the composition range 32 to 82 at.% V, as well as the thermodynamic curves of Kubaschewski *et al.* [77Kub], are all in close accord with the liquidus and solidus curves of Fig. 1.

A complete range of solid solubility in the α phase at elevated temperatures has been verified by X-ray diffraction [29Osa, 30Wev, 54Ros]. Even at compositions where the σ phase tends to form, it has been found that the α phase may readily be retained by quenching. Complete solid solubility in the α phase is compatible with the atomic size difference of 6% [45Hum].

**γ Loop.** Early investigations were made of the effects of V additions on the allotropic transformations of Fe [06Put, 09Por], but Maurer [25Mau] seems to have been the first to recognize that such additions resulted in a closed γ loop. A large number of subsequent investigations [30Wev, 31Vog, 30Oya, 31Hou, 34Abr, 54Luc, 64Han, 65Han, 60Lis, 70Kir, 70Fis, 73Kov1, 73Kov2] involved the determination of the boundaries of this loop with results that, particularly among earlier work, showed appreciable scatter with reported values for the maximum V content within the loop varying between 1.2 and 2.7 at.% V. This scatter was largely attributable to variations in impurity levels. As an example, carbon content was shown [31Hou] to have an appreciable effect on the width of the γ-phase field, with the apparent width increasing with increasing carbon content because of the formation of a carbide phase. As a second example, contamination resulting from melting alloys in air [54Luc] led to a minimum in the γ loop at ~0.2 at.% V near 896 °C.

Within the past two decades, V of higher purity has become available. Within this more recent period, studies of the boundary of the γ loop show considerably less scatter, with the three most recent reports all showing the maximum V content as occurring near 1150 °C, with values of 1.41 at.% V [65Han], 1.39 at.% V [73Kov1], and 1.40 at.% V [70Fis]. Beyond the γ maximum, these same investigators found the α + γ two-phase field extending, respectively, to 1.81, 1.8, and 2.0 at.% V. Andersson [83And] quoted unpublished results of Kirchner and Gemmel [70Kir], which are in accord with the results of these investigations. For Fig. 1, values of 1.40 at.% V for the γ maximum and 2.0 at.% V for the upper limit of the two-phase field were taken from the work of Fischer *et al.* [70Fis]; this selection was made because of the purity of the alloys of Fischer *et al.* and because the magnetic technique which was employed allowed good resolution of the respective contributions of the ferritic and austenitic fractions in the two-phase field.

Hanneman *et al.* [64Han, 65Han] made lattice parameter measurements as a function of temperature to determine the volumetric changes associated with the $\alpha \rightarrow \gamma$ transformation and examined the effects of pressure on the transformation with pressures to 50 kbar. They found that a 1.01 at.% V alloy at ambient pressure contracted by 0.069 $cm^3$/mol $Fe_{0.9899}V_{0.0101}$ upon being heated through the transformation. Continued heating caused a reversion of the transformation on the upper side of the γ loop with an expansion of 0.048 $cm^3$/mol $Fe_{0.9899}V_{0.0101}$. They found that the γ loop expands with increasing pressure, and their contours for the loop at representative pressures are shown in Fig. 2.

**σ Phase.** Wever and Jellinghaus [30Wev] were the first to report an intermediate phase in the Fe-V system, and it was soon recognized [31Wev, 48And] that this phase was isomorphous with the intermediate σ phase in the Fe-Cr system. Subsequent studies [50Pie, 51Pea, 51Sul, 54Gre] showed that these two Fe-V and Fe-Cr phases were members of a more numerous group of transition metal-transition metal phases that have become generally known as σ phases. Interpretation of X-ray diffraction patterns to determine the crystallography of these phases was initially hampered by the fact that the atomic scattering factor for X-rays of the transition elements V, Cr, Mn, Fe, Co, and Ni are all closely comparable. Shoemaker and Bergman [50Sho] used single-crystal X-ray techniques to determine the lattice parameters, space group, and the fact that there were 30 atoms per unit cell for σ Fe-Cr. Martens and Duwez [52Mar] studied the Fe-Cr-V ternary system and were able to show that the σ phase was continuous from the binary Fe-Cr side to the binary Fe-V side. They utilized the data from Shoemaker and Bergman to choose lattice parameters for the Fe-Cr side and to follow these parameters across the compositional range to obtain the first correct lattice parameters for the binary σ Fe-V phase. Kasper and Waterstrat [56Kas] subsequently used neutron diffraction techniques to determine the occupancy of the crystallographic sites by the Fe and V atomic species.

In 1950 Pearson [50Pea] commented that the boundaries of the σ phase in the Fe-V system were not known with great accuracy, and though the recent data of Inden and Büth [83But] have improved the situation, some uncertainties still persist. For instance, it is accepted that the congruent $\alpha \rightleftarrows \sigma$ transformation occurs near equiatomic stoichi-

**Fig. 3 Comparison of the Calculated vs Experimental $\alpha/\sigma$ Equilibria**

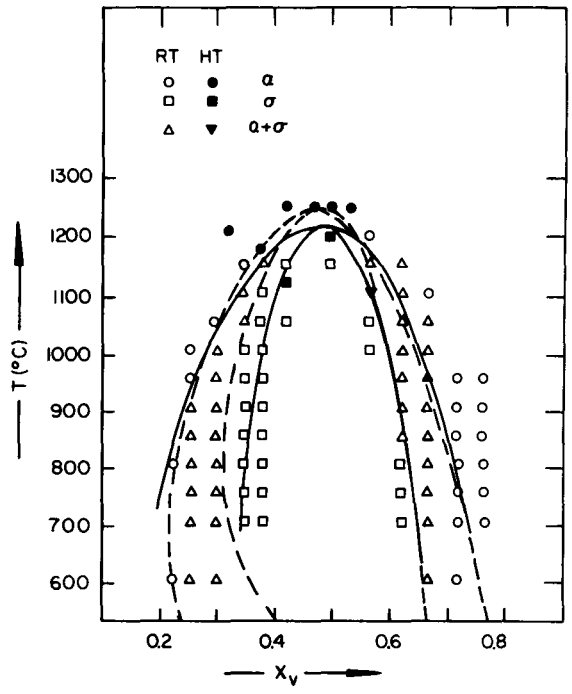


——— ≡ Hack *et al.* [79Hac]; — — — — ≡ Andersson [83And]. ○ ≡ measurements on quenched specimens and ● ≡ measurements made at temperature, from Chiriac and Inden [79Chi].
J. F. Smith, 1984.

ometry, but the temperature of the transformation has been reported over a wide range: below 1200 °C [Hansen], 1234 °C [30Wev], 1219 °C [79Hac], 1225 °C [62Mat], 1225 °C [79Chi], 1170 °C [73Mal], 1246 °C [83And], and 1247 °C [83But].

Boundaries for the homogeneous $\sigma$-phase field at lower temperatures were variously reported ~30 to ~58 at.% V near 1000 °C [30Wev], ~37 to ~57 at.% V at 700 °C [52Mar], ~39 to ~54.5 at.% V at 1075 °C [54Gre], and ~34 to ~53 at.% V without temperature specification [59Stu]. At 700 °C [52Mar], the boundary of the $\alpha$ phase on the Fe-rich side was reported as ~24 at.% V and on the V-rich side as ~66 at.% V. Again, at 700 °C, Hanneman *et al.* [65Han] in a study of pressure effects found, on the Fe-rich side, that the $\alpha$ phase extended to ~26 at.% V and the $\sigma$ phase was homogeneous beyond ~35 at.% V, and at 40 kbar, these values were shifted, respectively, to ~19 and ~30 at.% V. The same change in pressure was indicated as raising the temperature of the congruent $\alpha \rightleftarrows \sigma$ transformation from just above 1200 to ~1300 °C.

Unpublished data from Chiriac and Inden [79Chi] for the boundaries associated with the $\alpha \rightleftarrows \sigma$ transformation are shown in Fig. 3 for a grid of 12 compositions by 13 temperatures; long term anneals were used to ensure equilibration. The open points in the figure represent data based on room-temperature-examination post annealing, and the solid points represent data taken at temperature. The method of determining the number and type of phases in each alloy has been by X-ray diffraction, and graphical reproduction of the results are included in the reports of Hack *et al.* [79Hac], of Spencer [79Spe], and of Gallagher *et al.* [81Gal].

Variations in metal purity undoubtedly contribute to the diversity of results. The kinetics [59Bun] of the $\alpha \rightleftarrows \sigma$ transformation also play a role in defeating precise determination of the temperature-composition coordinates of the $\sigma$ and $\alpha + \sigma$ phase fields. The boundaries that are shown in Fig. 1 are the calculated boundaries of Inden and Büth [83But] and are based upon thermodynamic data with inclusion of effects from atomic and magnetic ordering. These calculated boundaries thus represent the prognosis for the temperature-composition coordinates after attainment of strain-free equilibrium in the pure binary system. For comparative purposes, Fig. 3 shows the calculated boundaries of Hack *et al.* [79Hac] and of Andersson [83And], together with the experimental data of Chiriac and Inden [79Chi].

**Magnetic Aspects ($\alpha$ Phase).** The Curie temperature of the $\alpha$ phase has been measured as a function of composition by a number of investigators [09Por, 10Hon, 25Mau, 30Oya, 30Wev, 31Vog, 34Abr, 36Fal] and, with a single exception [10Hon] that can be attributed to poor metal purity, there is agreement that V additions to Fe cause the Curie temperature of the $\alpha$ phase to pass through a maximum above 800 °C and below 20 at.% V. The maximum in Fig. 1 between 13 and 14 at.% V near 840 °C is a compromise among the composite data. From studies at higher temperatures in the paramagnetic region, Arajs *et al.* [62Ara] placed the maximum of the paramagnetic Curie temperature at 880 °C and 10 at.% V; the difference between the ferromagnetic Curie maximum and the paramagnetic Curie maximum results from the neglect of curvature in the reciprocal susceptibility vs temperature plots immediately above the temperature intercept. The reasons for this curvature are not understood.

Fallot [36Fal], Nevitt and Aldred [63Nev], and Aldred [72Ald] have examined the saturation magnetization of alloys in the $\alpha$ phase as functions of composition and temperature. With minor differences which are noted, the three sets of data are in good accord. The data of Nevitt and Aldred [63Nev] were taken from samples quenched from above 1200 °C and, in the composition region where the $\sigma$ phase tends to form, control specimens for metallographic analyses and X-ray diffraction were processed together with the magnetic samples to verify that the processing produced $\alpha$-phase alloys. Data from the magnetic samples for the composition range $0 \leq X_V \leq 0.62$ yielded the relationship:

$$\overline{\mu}_B = 2.232 - 3.286\, X_V$$

where $\overline{\mu}_B$ is the average number of Bohr magnetons per atom of alloy, and $X_V$ is the mole fraction of V. (Note: The trend of moment with composition has curvature if the relationship is shifted to the number of Bohr magnetons per Fe atom.)

Below 15 at.% V, the experimental points of Fallot [36Fal] fall essentially on this line, but three points above 15 at.% V drift below the linear relationship, and this deviation is believed attributable to incomplete retention of the $\alpha$ phase. Aldred [72Ald] reported data for the composition range 0 to 25.2 at.% V, and, in the range 6.1 to 25.2 at.% V, Aldred's experimental points are all within 1.5% of the linear relationship of Nevitt and Aldred

[63Nev]. Below 6.1 at.% V, however, Aldred's data show a slight curvature that may be represented as:

$$\bar{\mu}_B = 2.217 - 2.676\, X_V - 5.16\, X_V^2$$

Nevitt and Aldred [63Nev] noted the possibility of curvature in this low-concentration region, and this curvature brings the intercept moment per atom into agreement with the generally accepted moment for pure Fe. It is also worthy of comment that individual atomic moments of the order of $-1\ \bar{\mu}_B$ for V and 2.0 to 2.2 $\bar{\mu}_B$ for Fe were determined [82Mir1] by neutron diffraction with alloys in the composition range 0 to 25 at.% V. These moments, when averaged for composition, are in reasonable accord with the saturation magnetization data.

The linear equation for $\bar{\mu}_B$ should become zero at $X_V = 0.679$. The data of Nevitt and Aldred [63Nev] showed that, above $X_V = 0.62$, the moments rise above the linear extrapolation, tending toward zero at $X_V \geq 0.70$. This behavior is undoubtedly correlated with the observation that there is residual short-range magnetic order at low temperatures in alloys with V concentrations above $X_V = 0.70$. From low-temperature heat capacity data for alloys near this composition, Cheng *et al.* [60Che] and Scurlock and Wray [63Scu] found pronounced deviations from linearity in plots of $C_p/T$ vs $T$. The non-linear contribution has been interpreted as arising from magnetically ordered clusters without long-range order [60Che, 61Sch, 63Scu]. Claus [75Cla] measured ac susceptibilities to determine the onset of magnetic ordering as 16.8 K in an alloy with $X_V = 0.705$ and as 4.2 K in an alloy with $X_V = 0.715$, with significant differences in the magnetization depending on whether or not cooling through the ordering temperature was in a magnetic field. This behavior is indicative of the existence of giant spin clusters in these alloys, and such spin clusters are associated with superparamagnetism [68Hah] and with the spin glass state [78Myd].

**$\alpha'$ Phase.** The $\alpha'$ phase is a metastable phase with the CsCl structure; conditions which lead to the formation of the phase are discussed in the next section of this evaluation. Nevitt and Aldred [63Nev] measured the saturation magnetization of this phase at four alloy compositions: $X_V = 0.400$, $X_V = 0.470$, $X_V = 0.549$, and $X_V = 0.618$. They found the magnetic moments of the $\alpha'$ phase tended to be lower than the moments of the $\alpha$ phase, with the difference amounting to about 0.4 $\bar{\mu}_B$ near equiatomic stoichiometry. Values for their four alloy compositions have been read with limited precision from their graph of one column width, respectively, as 1.25, 0.93, 0.75, and 0.50 $\bar{\mu}_B$ per Fe atom. Chandross and Shoemaker [62Cha] used neutron diffraction to evaluate a magnetic moment of 0.7 $\bar{\mu}_B$ per Fe atom for an alloy with $X_V = 0.533$. This value is in good accord with the value of 0.75 $\bar{\mu}_B$ per Fe atom found by Nevitt and Aldred [63Nev] for the composition of $X_V = 0.549$.

**$\sigma$ Phase.** Nevitt and Beck [55Nev] initially reported a Curie temperature of 203 K for the $\sigma$ phase whose alloy composition was $X_V = 0.524$. Parsons [60Par] found Curie temperatures to be somewhat lower, with values of 130 K for $X_V = 0.422$, 72 K for $X_V = 0.455$, 44 K for $X_V = 0.480$, and 40 K for $X_V = 0.50$. Spontaneous magnetization data for the $\sigma$ phase from Parsons [60Par] and from Nevitt and Aldred [63Nev] fall on a single straight line when plotted against at.% V. The mean magnetic moments in Bohr magnetons per atom of alloy were reported as 0.261 for 42.2 at.% V, 0.177 for 45.5 at.% V, 0.110 for 48.0 at.% V, and 0.091 for 50 at.% V by Parsons [60Par] and 0.29 for 40.0 at.% V and 0.14 for 47.0 at.% V by Nevitt and Aldred [63Nev]. These moments are about a factor of three lower than those of the $\alpha$ and $\alpha'$ phases. These moments extrapolate to zero between 53 and 54 at.% V, and experimental tests on a 54.9 at.% V alloy by Nevitt and Aldred [63Nev] confirmed that it is not ferromagnetic in the $\sigma$ phase.

**High-Pressure and Metastable Phases.** Loree [64Lor] checked for pressure-induced transformations in Fe-V alloys by applying explosive shock loads. He found that the high-pressure transformation, which occurs in Fe near 130 kbar and is thought to be a bcc → cph transformation, also occurs in Fe-V alloys. In an 11 at.% V alloy, the requisite pressure for the transformation was found to be 250 kbar, and the transformation was accompanied by a volume contraction of ~5%. The requisite pressure was reported to rise rapidly with increasing V content to exceed 500 kbar at compositions in the range 21 to 27 at.% V.

A metastable $\alpha'$ phase with the CsCl structure has been observed at compositions in the central portion of the Fe-V system. This phase is apparently competitive with, but less stable than, the $\sigma$ phase; however, the kinetics are such that $\alpha'$ can form before $\sigma$ at temperatures below 700 °C. At room temperature, the kinetics of $\alpha \rightarrow \alpha'$ and of $\alpha \rightarrow \sigma$ are so slow that $\alpha$ itself can be retained by quenching from temperatures above the stability limit of the $\sigma$ phase. This was recognized early [30Wev], and quenched specimens were utilized to obtain lattice parameters for the $\alpha$ phase across the complete composition range. In fact, the low-temperature kinetics of the $\alpha \rightarrow \sigma$ transformation are so sluggish that Dwight [59Dwi], in a survey of binary V systems for $\sigma$ phases, found only the bcc structure of the $\alpha$ phase with no $\sigma$ in the Fe-V system; his choice of X-radiation, Co K$\alpha$ and Cu K$\alpha$, would not distinguish $\alpha'$ from $\alpha$. The kinetic studies of Bungardt and Spyra [59Bun] showed that above 700 °C, the $\alpha \rightarrow \sigma$ transformation proceeds directly, but below 700 °C, the $\alpha'$ phase occurs as a metastable intermediate.

A number of investigations [56Bec, 57Phi, 63Nev] showed that initial quenching from above 1200 °C to retain the $\alpha$ phase, followed by annealing for a few hours at 600 to 625 °C, caused the appearance of the $\alpha'$ phase. Specifically, with Cr K$\alpha$ radiation, the superlattice lines (100), (111), and (210) appeared after such heat treatment and were superimposed over the regular $h + k + l = 2n$ lines in the powder diffraction patterns. The wavelength of Cr K$\alpha$ radiation lies between the V and Fe absorption edges and makes possible the distinguishing of the V diffraction contribution from the Fe diffraction contribution. A neutron diffraction study [62Cha] of a 53.3 at.% V alloy, which was homogenized at 1250 °C, quenched, and then annealed for 6 h at 600 °C, showed the atomic ordering to be ~77% complete with 17.3% V and 82.7% Fe atoms on sites of type 1 and 89.3% V and 10.7% Fe atoms on sites of type 2. Dilatometry, thermal analyses, and microhardness data also corroborate $\alpha \rightarrow \alpha'$ ordering in the central portion of the Fe-V system [64Dai].

Zakharova and co-workers [57Zak, 58Zak, 59Zak], in a series of papers, reported the existence of an fcc phase in the central portion of the system. They followed the procedure of quenching from above 1200 °C and then annealing near

**Table 1 Fe-V Crystal Structure Data**

| Phase | Composition(a), at.% V | Pearson symbol | Space group | Prototype |
|---|---|---|---|---|
| ($\alpha$Fe) or (V) or $\alpha$ | 0 to 100 | *cI2* | *Im3m* | W |
| ($\gamma$Fe) or $\gamma$ | 1.01 | *cF4* | *Fm3m* | Cu |
| $\sigma$ | 29.6 to 60.1 | *tP30* | $P4_2/mnm$ | $\sigma$Cr-Fe |
| **Metastable phase** | | | | |
| $\alpha'$ | 50 | *cP2* | *Pm3m* | CsCl |

(a) From the phase diagram.

**Table 2 Fe-V Lattice Parameter Data**

| Phase | Composition, at.% V | Lattice parameters (a), nm *a* | *c* | Reference |
|---|---|---|---|---|
| ($\alpha$Fe) or (V) or $\alpha$ | 0 | 0.2866 | ... | (b) |
| | 10 | 0.2877 | ... | |
| | 20 | 0.2888 | ... | |
| | 30 | 0.2898 | ... | |
| | 40 | 0.2908 | ... | |
| | 50 | 0.2920 | ... | |
| | 60 | 0.2933 | ... | |
| | 70 | 0.2949 | ... | |
| | 80 | 0.2968 | ... | |
| | 90 | 0.2994 | ... | |
| | 100 | 0.3032 | ... | |
| ($\gamma$Fe) or $\gamma$ | 1.01 | 0.36543(c) | ... | [64Han] |
| | | 0.36631(d) | ... | |
| | | 0.36717(e) | ... | |
| $\sigma$ | 29.6 | 0.8865 | 0.4605 | [64Han] |
| | 34 | 0.8866 | 0.4598 | [59Stu] |
| | 40.4 | 0.8915 | 0.4615 | [64Han] |
| | 49.9 | 0.8956 | 0.4627 | [64Han] |
| | 50.0 | 0.895 | 0.462 | [52Mar] |
| | 52 | 0.8963 | 0.4629 | [52Pea] |
| | 53 | 0.8978 | 0.4629 | [59Stu] |
| | 60.1 | 0.9015 | 0.4642 | [64Han] |
| $\alpha'$ (f) | 50 | 0.2910 | ... | [57Phi] |

(a) Data from Hanneman and Mariano [64Han] for a 1 at.% V alloy show lattice parameters to have the following temperature dependences:
$\alpha$ phase: $a_T$(nm) = 0.28661 + 4.297 × $10^{-6}$ $T$(°C); 25 °C ≤ $T$ ≤ 925 °C
$\gamma$ phase: $a_T$(nm) = 0.36016 + 8.75 × $10^{-6}$ $T$(°C); 925 °C ≤ $T$ ≤ 1375 °C
(b) Data from Fig. 4. (c) At 1000 °C. (d) At 1100 °C. (e) At 1200 °C. (f) Metastable phase.

**Fig. 4 Room-Temperature Lattice Parameters of the $\alpha$ Phase as a Function of Composition**

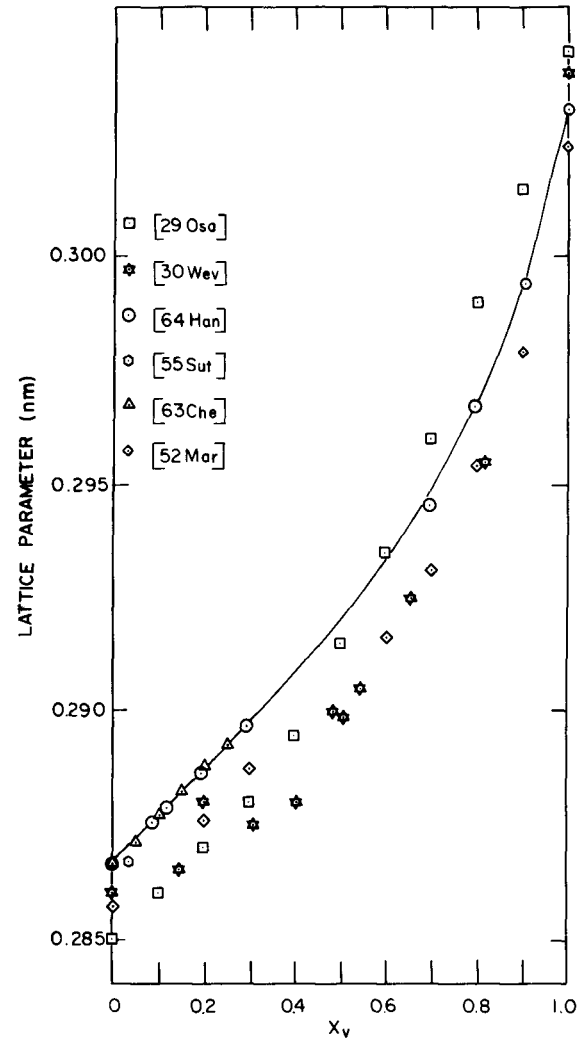


Data from a number of investigators, with the solid line representing the data of best precision. J. F. Smith, 1984.

600 °C, but instead of $\alpha'$, they found two-phase alloys: $\alpha + \beta$, with $\beta$ being the fcc phase. In view of the high carbon and silicon content of their unalloyed V, and with no subsequent corroboration, it is most likely that their fcc phase is not a binary Fe-V phase, but is an impurity effect.

It was noted earlier, under the section on Phase Relationships, that Hanneman *et al.* [64Han, 65Han] had studied the effects of pressure on the $\alpha \rightarrow \gamma$ transformation and on $\sigma$ phase stability with pressures from ambient to 50 kbar. The study of the $\alpha \rightarrow \gamma$ transformation made use of diffusion couples at high temperatures and high pressures with subsequent microprobe analyses. It was established that the $\gamma$ loop expanded with increasing pressure. The study of the $\sigma$ phase stability made use of equilibrations at various pressures and temperatures followed by quenchings under pressure. X-ray powder patterns at ambient pressure were then used to determine the phases present in the quenched specimens. It was found that both the temperature range and composition range of stability of the $\sigma$ phase increased with increasing pressure.

## Crystallography

**$\alpha$ Solid Solution.** The continuous solid solution, which extends across the Fe-V system at elevated temperatures, has the bcc structure for which W is the prototype. (Crystal structure data are given in Table 1.) Data for the lattice parameters [29Osa, 30Wev, 52Mar, 55Sut, 63Che, 64Han] are plotted as a function of composition in Fig. 4. The values of Chessin *et al.* [63Che] and of Hanneman and Mariano [64Han] were determined with superior precision, and a smooth curve is drawn through their experimental points. Lattice parameter values from this smooth curve for the $\alpha$ phase are listed in Table 2. All data in Fig. 4 show negative deviation from Vegard's rule, and this is consistent with indications of short-range order that have been found by Sedykh [78Sed] in a 25 at.% V alloy, by Mirebeau *et al.* [82Mir2] with alloys in the composition range 1 to 20 at.% V, and by Bokshtein and Guglya [79Bok] in the composition range 2.5 to 10 at.% V. These studies were done with a combination of Mössbauer

**Table 3 Atom Positions and Occupancy by Fe and V Atoms for the σFe-V Phase in Fe-V, with Space Group Symmetry $P4_2/mnm$**

| Set No. | Atom set | Positional parameters | Number of atoms Fe | V |
|---|---|---|---|---|
| I | 2*b* | Parameterless | 1.7 | 0.3 |
| II | 4*f* | $x = 0.103$ | 0 | 4 |
| III | 8*i* | $x = 0.371$; $y = 0.037$ | 1.5 | 6.5 |
| IV | 8*i* | $x = 0.566$; $y = 0.024$ | 6.8 | 1.2 |
| V | 8*j* | $x = 0.316$; $z = 0.250$ | 2 | 6 |

spectroscopy and neutron analysis [78Sed, 79Bok], and with nuclear magnetic resonance and neutron scattering [82Mir2].

Hanneman and Mariano [64Han] measured the lattice parameter of a 1.01 at.% V alloy as a function of temperature. In the range between room temperature and the bottom of the γ loop, their data are adequately described by the relationship:

$$a_T(\text{nm}) = 0.28661 + 4.297 \times 10^{-6} T\ (°\text{C})$$

**γ Phase.** Hanneman and Mariano [64Han] measured the lattice parameter of the fcc γ phase in a 1.01 at.% alloy at temperatures of 1000, 1100, and 1200 °C. This phase has the fcc structure for which Cu is the prototype. Within the γ loop, the lattice parameters of the 1.01 at.% alloy are adequately described by the relationship:

$$a_T(\text{nm}) = 0.36016 + 8.75 \times 10^{-6} T\ (°\text{C})$$

**Metastable α′ Phase.** Philip and Beck [57Phi] quenched a nominally equiatomic alloy from 1250 °C and, for the as-quenched α phase, found a lattice parameter of $a = 0.2928$ nm. After annealing at 625 °C for 1 h, superlattice lines were observed, and the lattice parameter of the ordered α′ phase was found to be $a = 0.2910$ nm. These lattice parameters indicate that atomic ordering in the central portion of the system produces a volume contraction of ~1.8%.

**σ Phase.** Lattice parameters for the σ phase in the Fe-V system are shown for a number of compositions in Table 2. This phase crystallizes with space group symmetry $P4_2/mnm$ and has thirty atoms per unit cell distributed among five sets of crystallographically distinguishable sites. Kasper and Waterstrat [56Kas] used neutron diffraction to determine the statistical occupancy by Fe and V atoms of the five different sets from an alloy with $X_V = 0.60$. The results are summarized in Table 3.

## Thermodynamics

**Thermodynamics of Phase Formation.** Six independent investigations of vapor pressures over Fe-V alloys were made with the Knudsen effusion method. Saxer [62Sax] used the weight loss technique with solid alloys across the composition range at temperatures between 1289 and 1451 °C (1562 and 1724 K). Myles and Aldred [64Myl] used the torsion effusion technique with solid alloys across the composition range at temperatures between 1178 and 1547 °C (1451 and 1820 K). Weidner [71Wei], Furukawa and Kato [75Fur], Robinson and Argent [76Rob], and Kubaschewski *et al.* [77Kub] all used the mass spectrometric technique. Weidner [71Wei] examined solid alloys in the composition range $0.10 \le X_V \le 0.25$ and liquid alloys in the composition range $0.295 \le X_V \le 1$ at a temperature of 1600 °C (1873 K); Furukawa and Kato [75Fur] worked at the same temperature and at essentially the same compositions; Robinson and Argent [76Rob] examined two solid alloys at $X_V = 0.0508$ and $X_V = 0.0999$ at 1550 and 1650 °C (1823 and 1923 K), and Kubaschewski *et al.* [77Kub] examined liquid alloys through the composition range at 1920 °C (2193 K).

Fruehan [70Fru] used an emf technique with solid oxide electrolytes to determine the Gibbs energies of formation of liquid alloys in the composition range $0 \le X_V \le 0.40$ at 1600 °C (1873 K). Ilyuschenko *et al.* [81Ily] used an emf technique with liquid chloride and liquid bromide electrolytes to measure the activities of solid alloys at compositions of $X_V = 0.8$ and $X_V = 0.9$, and Balkovoi *et al.* [82Bal] measured the activity of V in liquid alloys in the composition range $0 \le X_V \le 0.55$. Ilyuschenko showed that emf measurements on these alloys are complicated by the fact that both V and Fe tend to change valence state.

Evaluations of the enthalpies of alloy formation were made by adiabatic calorimetry by Spencer and Putland [73Spe] for the composition range $0.40 \le X_V \le 0.58$ near 1350 °C (1623 K), and by Malinsky and Claisse [73Mal] for an alloy with $X_V = 0.48$ at temperatures ranging from 1000 to 1157 °C (1237 to 1430 K). A calorimetric measurement of the partial molal enthalpy of solution of V in bcc Fe at infinite dilution was made at 1600 °C (1873 K) by Dyubanov [75Dyu]. Calorimetric measurements of the enthalpies of liquid alloy formation were made by Batalin *et al.* [81Bat, 82Bat] for $X_V \le 0.61$ at 1657 °C (1930 K) and by Iguchi *et al.* [82Igu] at 1600 °C (1873 K).

Enthalpies and entropies of alloy formation from the vapor pressure and emf measurements show appreciable scatter, with values at some compositions differing by order of magnitude and even by sign. In contrast, the calorimetric data of Spencer [73Spe] and of Malinsky and Claisse [73Mal] are in good accord. This agrees with the widely accepted view that calorimetric heats are normally to be preferred to heats obtained by second law evaluations. Among the Gibbs energy data, the data of Kubaschewski *et al.* [77Kub] are preferred because:

- Measurements were extended to very low concentrations of Fe and of V within the same phase field
- Measurements were made at temperatures high enough to obviate kinetic inhibition of equilibrium
- Vapor pressures at the higher temperatures were higher and thus could be measured with better precision

These considerations, when combined with the fact that the enthalpy measurements of Batalin *et al.* [81Bat, 82Bat] and of Iguchi *et al.* [82Igu] were not yet available, make quite reasonable the selection of the enthalpy data of Spencer and Putland [73Spe], and the Gibbs energy data of Kubaschewski *et al.* [77Kub], by Hack *et al.* [79Hac], and by Andersson [83And], as the bases for the development of self-consistent sets of thermodynamic functions for calculating the phase equilibria in the system.

Hack *et al.* [79Hac] developed expressions for the enthalpies and excess entropies of alloy formation in the form:

$$\Delta H^i \quad \text{or} \quad {}^E\Delta S^i = X_V X_{Fe} \Sigma_n a_n (X_V - X_{Fe})^n$$

**Table 4 Coefficients for the Expression [79Hac]**
**$\Delta H^i$ or ${}^E\Delta S^i = X_V X_{Fe} \Sigma a_n (X_V - X_{Fe})^n$**
**in units of J/mol $Fe_{1-x}V_x$ for $\Delta H^i$ and J/K mol $Fe_{1-x}V_x$ for ${}^E\Delta S^i$**

| Quantity | Coefficients $a_0$ | $a_1$ | $a_2$ | $a_3$ | $a_4$ |
|---|---|---|---|---|---|
| $\Delta H^\alpha$ | −22 853.0 | −6715.32 | −1221.31 | ... | ... |
| $\Delta H^\sigma$ | −56 504.9 | −6715.32 | −1221.31 | ... | ... |
| $\Delta H^L$ | −22 853.0 | −6715.32 | −1221.31 | ... | ... |
| ${}^E\Delta S^\alpha$ | −6.58018 | 3.90813 | 3.80540 | −2.17985 | −2.46840 |
| ${}^E\Delta S^\sigma$ | −14.7848 | 3.90813 | 3.80540 | −2.17985 | −2.46840 |
| ${}^E\Delta S^L$ | −2.44555 | 3.99703 | 3.02038 | −2.88091 | −3.06407 |

for the generalized reaction:

$$(1 - x)Fe^i + xV^i \rightarrow (Fe_{1-x}V_x)^i$$

where $i$ designates the $\alpha$, $\sigma$, or L phase. Coefficients for the enthalpies and excess entropies for the three reactions are listed in Table 4. The $\alpha$/L and $\alpha/\sigma$ phase boundaries were calculated by combining these functions with the lattice stability relations:

$$Fe(\alpha, \delta) \rightarrow Fe(L): \quad \Delta G_{Fe}^{\alpha \rightarrow L} = 1.38072 \times 10^4 - 7.63162\,T$$

$$V(\alpha) \rightarrow V(L): \quad \Delta G_{V}^{\alpha \rightarrow L} = 1.82422 \times 10^4 - 8.36800\,T$$

$$Fe(\alpha, \delta) \rightarrow Fe(\sigma): \quad \Delta G_{Fe}^{\alpha \rightarrow \sigma} = 4.60328 \times 10^3 + 0.22589\,T$$

$$V(\alpha) \rightarrow V(\sigma): \quad \Delta G_{V}^{\alpha \rightarrow \sigma} = 5.94965 \times 10^3 + 0.15604\,T$$

where the numerical values for the fusion reactions have been taken from Kaufman and Bernstein [70Kau] and the values for the hypothetical $\alpha \rightarrow \sigma$ transformations from Bernard [79Ber]. Use of alternative expressions such as those of Hayes and Kubitz [79Hay] for the $\alpha \rightarrow \sigma$ transformations of pure Fe and pure V should not significantly modify the calculated results.

Hack *et al.* [79Hac] did not develop relationships for describing the $\alpha/\gamma$ phase equilibria, because Hack's formulation of the Gibbs energies of phase formation neglected magnetic contributions. Recently, Andersson [83And], starting with essentially the same thermodynamic input as Hack *et al.*, added expressions for the magnetic contributions to the Gibbs energies of phase formation and recalculated the entire diagram with fewer adjustable parameters. He used a three-sublattice model for the $\sigma$ phase. The details of his calculation are too involved for inclusion in the present review, but it may be noted that the compositions associated with the $\alpha$/L and V-rich side of the $\alpha/\sigma$ equilibria are not much affected by introduction of the magnetic energy. However, addition of the magnetic energy causes the compositions associated with the $\alpha/\sigma$ equilibria on the Fe-rich side to have a significantly different temperature trend; Andersson's boundaries for the $\alpha/\sigma$ equilibria are shown by dashed lines in Fig. 3. The introduction of the magnetic energy also allows calculation of the boundaries for the $\alpha/\gamma$ equilibria, and Andersson's results are reproduced in Fig. 5. Inden and Büth's [83But] evaluation of the entire system takes into account both chemical and magnetic ordering; however, Büth's complete thesis is not yet available to this reviewer, so that explicit analytical expressions for the Gibbs energy functions are not given here.

**Fig. 5 Comparison of the Calculated vs Experimental Phase Boundaries for the $\alpha/\gamma$ Equilibria**

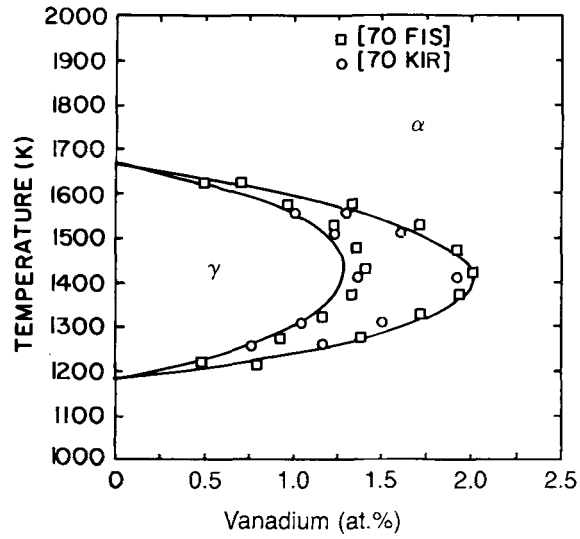


——— ≡ Andersson [83And]; □ ≡ Fischer *et al.* [70Fis]; ○ ≡ Kirchner and Gemmel [70Kir]. J. F. Smith, 1984.

Hanneman *et al.* [65Han] calculated the $\alpha/\gamma$ equilibria as a function of pressure. For tractability, they introduced a number of simplifying, but reasonable, assumptions. The reader is referred to the original publication for details. They used four items of empirical information as input. Two of these items were from ambient pressure data. The first consists of the temperature dependence of the ambient pressure values for $X_V^\alpha$ and $X_V^\gamma$ which are the compositions at the termini of the $\alpha$ and $\gamma$ phase fields; these values were taken from the ambient pressure diagram. The second item was the volume change associated with the $\alpha \rightarrow \gamma$ transformation of pure Fe as a function of temperature from the lattice parameter data of Basinski [Pearson 1]. For the third item, Hanneman *et al.* [65Han] took the formulation of Kaufman *et al.* [63Kau] for the pressure and temperature dependence of the Gibbs energy change associated with the $\alpha \rightarrow \gamma$ transformation. For the fourth item, the mean volume variation of the $\alpha$ and $\gamma$ phases as a function of composition was evaluated as 0.6 $cm^3$/unit mole fraction from high-temperature X-ray measurements of Hanneman and Mariano [64Han]. With these data as input for the calculation, agreement between calculated and experimental points for $X_V^\alpha$ and $X_V^\gamma$ was

better than 0.005 for all experimental points at the 20, 40, and 50 kbar pressures of measurement.

**High-Temperature Heat Capacities.** Heat capacity data for the regime above room temperature have been accumulated from adiabatic calorimetry [67Sch, 73Spe, 73Mal, 76Nor] and from heat content measurements [65Rap, 67Sch, 73Ore]. Values are compared in Table 5, and in most instances, the original data were presented in graphical form and could be read with only limited precision, ~ ±0.3 to ±0.4 J/K·mol $Fe_{1-x}V_x$. It may be noted that at room temperature the heat capacity is essentially independent of composition, but at elevated temperature the magnetic disordering and the phase transitions produce systematic drifts with composition. A summary of thermodynamic data for the various transitions is shown in Table 6.

**Low-Temperature Heat Capacities.** Nitikin *et al.* [66Nit] found that nuclear hyperfine contributions from $V^{51}$ nuclei are substantial in the very-low-temperature range, 0.03 K ≤ $T$ ≤ 0.15 K, in Fe-rich ferromagnetic alloys with $X_V$ = 0.044 and $X_V$ = 0.138. Brewer *et al.* [64Bre] also found such a contribution in an alloy with $X$ = 0.10 from measurements in the temperature range 0.4 K ≤ $T$ ≤ 7 K, but the relative magnitude of the contribution with respect to the lattice and electronic contributions decreased with increasing temperature, and above 1 K, only the $T$ and $T^3$ terms were found meaningful. The insignificance of the nuclear hyperfine contribution at temperatures much above 1 K is corroborated by the attempt by Wei *et al.* [61Wei] to resolve such a contribution from the heat capacity measurements of Cheng *et al.* [60Che] on an alloy with $X_V$ = 0.33 at temperatures between 1.4 and 4.2 K; meaningful resolution was masked by the experimental uncertainty in the data.

An extensive set of low-temperature heat capacities was measured by Cheng *et al.* [60Che] at temperatures between 1.4 and 4.2 K and at compositions through the range 0.33 ≤ $X_V$ ≤ 0.92. They found that data for alloys with compositions 0.33 ≤ $X_V$ ≤ 0.66 and 0.80 ≤ $X_V$ ≤ 0.92 could be adequately fit by equations of the type:

$$C = \gamma T + \beta T^3$$

where the linear term is the electronic contribution, and the cubic term is the lattice contribution. However, for alloys in the range 0.69 ≤ $X_V$ ≤ 0.78, an additional tem-

**Table 5 Experimental Values for the Heat Capacities of Fe-V Alloys**

| Temperature, K | Heat capacity, J/K·mol $Fe_{1-x}V_x$ Composition, at.% V | | | | | | | | | | | | | |
|---|---|---|---|---|---|---|---|---|---|---|---|---|---|---|
| | 0 (a) | 0.52 [76Nor] | 1.15 [76Nor] | 2.18 [76Nor] | 14 [73Ore] | 16.5 [65Rap] | 30 [73Ore] | 48 [73Mal] | 49 [65Rap] | 50 [73Spe] | 73 [67Sch] | 85 [67Sch] | 87.6 [65Rap] | 92 [67Sch] |
| 298 | 24.98 | ··· | ··· | ··· | ··· | 25.0 | ··· | ··· | 24.9 | ··· | 25.1(b) | 24.7 | 24.9 | 25.9 |
| 400 | 27.36 | ··· | ··· | ··· | ··· | 26.0 | ··· | ··· | 25.6 | ··· | 27.0(b) | 26.2 | 25.6 | 26.9 |
| 500 | 29.71 | ··· | ··· | ··· | ··· | 27.4 | ··· | ··· | 26.5 | ··· | 28.3(b) | 27.4 | 26.4 | 28.1 |
| 600 | 32.05 | ··· | ··· | ··· | 30.5 | 29.0 | 28.1(b) | ··· | 27.2 | ··· | 30.7(b) | 28.8 | 27.4 | 29.3 |
| 700 | 34.60 | 35.4 | 34.6 | 35.3 | 33.2 | 32.0 | 31.8(b) | ··· | 28.4 | ··· | 32.3 | 29.9 | 28.5 | 30.5 |
| 800 | 37.95 | 38.1 | 36.6 | 37.2 | 36.9 | 36.5 | 36.2(b) | ··· | 30.0 | ··· | 33.0 | 29.4 | 29.5 | 30.7 |
| 900 | 43.10 | 43.4 | 42.4 | 38.6 | 41.5 | 42.8 | 46.2(b) | ··· | 31.9 | ··· | 33.5 | 30.2 | 31.1 | 32.1 |
| 1000 | 54.43 | 54.9 | 52.0 | 49.5 | 48.9 | 51.3 | 42.8 | ··· | 34.3 | ··· | 37.8 | 31.3 | 32.3 | 33.6 |
| | | $T_c$ | | | $T_c$ | | | | | | | | | |
| 1100 | 46.40 | 45.7 | 43.4 | 42.9 | 56.5 | 58.7 | 36.3 | 32.0 | 36.7 | ··· | 37.7 | 32.3 | 33.8 | 35.0 |
| | | α ⇄ γ | | | | | | | | | | | | |
| 1200 | 34.02 | 40.6 | 36.8 | 35.2 | 38.5 | 38.7 | 33.4 | 32.7 | 38.5 | ··· | 39.8 | 33.4 | 35.4 | 36.5 |
| 1300 | 34.85 | 36.5 | 36.0(b) | 33.9 | 35.1 | 38.2 | 33.1 | 33.5 | 40.8 | 34.0 | 42.0 | 34.5 | 38.5 | 37.9 |
| 1400 | 35.69 | 36.6 | 36.5 | 34.5 | 33.5 | 39.3 | ··· | 34.2 | 43.6 | 36.4 | ··· | ··· | ··· | ··· |
| | | | | | | | | α ⇄ σ | | | | | | |
| 1500 | 36.53 | 37.4 | 36.5 | 36.1 | ··· | 39.6 | ··· | 36.0 | 41.4 | 30.1 | ··· | ··· | ··· | ··· |
| 1600 | 37.36 | 37.6 | 37.4(b) | ··· | ··· | ··· | ··· | 38.6 | ··· | 36.1 | ··· | ··· | ··· | ··· |
| | | α ⇄ γ | | | | | | | | | | | | |
| 1700 | 41.46 | ··· | ··· | ··· | ··· | ··· | ··· | ··· | ··· | ··· | ··· | ··· | ··· | ··· |

(a) [Hultgren, Binary]. (b) Values may be applicable to two-phase material or to a metastable phase.

**Table 6 Transition Data with Enthalpies in J/mol $Fe_{1-x}V_x$ and Entropies and Heat Capacities in J/K·mol $Fe_{1-x}V_x$**

| Composition, at.% V | Curie temperature ($T_c$), K | $C_p(T_c)$ | $H^{Mag}$ | $S^{Mag}$ | Transitions $\Delta H^{\alpha\to\gamma}$ | $\Delta S^{\alpha\to\gamma}$ | $\Delta H^{\gamma\to\alpha}$ | $\Delta S^{\gamma\to\alpha}$ | $\Delta H^{\sigma\to\alpha}$ | $\Delta S^{\sigma\to\alpha}$ | Reference |
|---|---|---|---|---|---|---|---|---|---|---|---|
| 0.52 | 1046 | 85.8 | 6330 | 7.90 | 681 | 0.55 | 753 | 0.49 | ··· | ··· | [76Nor] |
| 1.15 | 1054 | 77.5 | 6060 | 7.56 | ··· | ··· | ··· | ··· | ··· | ··· | [76Nor] |
| 2.18 | 1063 | 69.2 | 5700 | 7.68 | ··· | ··· | ··· | ··· | ··· | ··· | [76Nor] |
| 14 | 1096 | 72.5 | ··· | ··· | ··· | ··· | ··· | ··· | ··· | ··· | [73Ore] |
| 16.5 | 1110 | 59.4 | ··· | ··· | ··· | ··· | ··· | ··· | ··· | ··· | [65Rap] |
| 30 | 997 | 58.9 | ··· | ··· | ··· | ··· | ··· | ··· | ··· | ··· | [73Ore] |
| 40 | ··· | ··· | ··· | ··· | ··· | ··· | ··· | ··· | 3011 | 2.13 | [73Spe] |
| 48 | ··· | ··· | ··· | ··· | ··· | ··· | ··· | ··· | 3155 | 2.21 | [73Spe] |
| 48 | ··· | ··· | ··· | ··· | ··· | ··· | ··· | ··· | 3230 | 2.23 | [73Mal] |
| 50 | ··· | ··· | ··· | ··· | ··· | ··· | ··· | ··· | 3130 | 2.19 | [73Spe] |
| 58 | ··· | ··· | ··· | ··· | ··· | ··· | ··· | ··· | 2156 | 1.59 | [73Spe] |

**Table 7 Parameters for Low-Temperature Heat Capacity Data for $Fe_{1-x}V_x$ in the Form**

$$C = \alpha T + \beta T^3 + \delta\left[\frac{\theta_E/T}{\exp(\theta_E/T) - 1}\right]^2 \exp(\theta_E/T) \quad \text{for Temperatures above 1 K}$$

| Composition, at.% V | Phase $\gamma$ (mJ/mol·K²) | $\beta$ (mJ/mol·K⁴) | $\delta$ (mJ/mol·K) | $\theta_E$ (K) | Temperature range, K | Reference |
|---|---|---|---|---|---|---|
| 10 | 3.38 | 0.0294 | 0 | ··· | 2 to 7 | [64Bre] |
| 33 | 3.61 | 0.0384 | 0 | ··· | 1.4 to 4.2 | [60Che] |
| 55 | 5.48 | 0.0196 | 0 | ··· | 1.4 to 4.2 | [60Che] |
| 66 | 6.99 | 0.0363 | 0 | ··· | 1.4 to 4.2 | [60Che] |
| 68 | 7.66 | 0.0156 | 3.97 | 5.55 | 1.5 to 16 | [79Ohl] |
| 70 | 7.12 | 0.0114 | 10.15 | 3.84 | 1.5 to 16 | [79Ohl] |
| 74 | 3.30 | 0.0177 | 4.7 | 0.002 | 1.5 to 16 | [79Ohl] |
| 80 | 3.83 | 0.0276 | 0 | ··· | 1.5 to 16 | [79Ohl] |
| 80 | 3.93 | 0.0147 | 0 | ··· | 1.4 to 4.2 | [60Che] |
| 85 | 5.11 | 0.0318 | 0 | ··· | 1.5 to 16 | [79Ohl] |
| 85 | 5.19 | 0.0166 | 0 | ··· | 1.4 to 4.2 | [60Che] |
| 90 | 6.35 | 0.0290 | 0 | ··· | 1.5 to 16 | [79Ohl] |
| 92 | 6.74 | 0.0279 | 0 | ··· | 1.4 to 4.2 | [60Che] |
| 95 | 7.66 | 0.0381 | 0 | ··· | 1.5 to 16 | [79Ohl] |
| 100 | 9.47 | 0.0427 | 0 | ··· | 1.5 to 16 | [79Ohl] |

perature dependence was evident. This additional contribution was interpreted by Schröder [61Sch] as being due to thermal oscillations of magnetic clusters with giant moments. This interpretation has been accepted and is consistent with subsequent data. Scurlock and Wray [63Scu] found the magnetic cluster contribution to occur in the composition range $0.68 < X_V < 0.78$, and Ohlendorf *et al.* [79Ohl] found $0.66 \leq X_V \leq 0.78$. The temperature dependence of the cluster contribution has been adequately represented by Einsteinian functions, so that the heat capacity data can be represented by:

$$C = \gamma T + \beta T^3 + \delta\left[\frac{\theta_E/T}{\exp(\theta_E/T) - 1}\right]^2 \exp(\theta_E/T)$$

where $\delta$ is proportional to the number of clusters per mole of metal. Values for the parameters at representative compositions are given in Table 7, with the mole referring to the formula $Fe_{1-x}V_x$ and with the data for pure V referring to the normal state.

## Cited References


**06Put:** P. Pütz, *Metall., 3,* 635-638, 649-656 (1906). (Equi Diagram; Experimental)

**08Vog:** R. Vogel and G. Tammann, *Z. Anorg. Chem., 58,* 79-82 (1908). (Equi Diagram; Experimental; #)

**09Por:** A. Portevin, *Rev. Metall., 6,* 1352-1355 (1909). (Equi Diagram; Experimental)

**10Hon:** K. Honda, *Ann. Phys., 32,* 1010-1011 (1910). (Equi Diagram; Experimental)

**25Mau:** E. Maurer, *Stahl Eisen, 45,* 1629-1632 (1925). (Equi Diagram; Experimental)

**29Osa:** A. Osawa and M. Oya, *Sci. Rep. Res. Inst. Tohoku Univ., 18,* 727-731 (1929). (Crys Structure, Equi Diagram; Experimental)

**30Oya:** M. Oya, *Sci. Rep. Res. Inst. Tohoku Univ., 19,* 235-245 (1930). (Equi Diagram; Experimental; #)

***30Wev:** F. Wever and W. Jellinghaus, *Mitt. Kaiser-Wilhelm Inst. Eisenforsch. Düsseldorf, 12,* 317-322 (1930). (Equi Diagram; Experimental; #)

**31Hou:** H. Hougardy, *Arch. Eisenhüttenwes., 4,* 497-503 (1931). (Equi Diagram; Experimental)

**31Vog:** R. Vogel and E. Martin, *Arch. Eisenhüttenwes., 4,* 487-495 (1931). (Equi Diagram; Experimental)

**31Wev:** F. Wever and W. Jellinghaus, *Mitt. Kaiser-Wilhelm Inst. Eisenforsch. Düsseldorf, 13,* 93-109, 143-147 (1931). (Crys Structure; Experimental)

**34Abr:** H. H. Abram, *J. Iron Steel Inst., 130,* 351-375 (1934). (Equi Diagram; Experimental)

**36Fal:** M. Fallot, *Ann. Phys., 6,* 305-387 (1936). (Equi Diagram; Experimental)

**45Hum:** W. Hume-Rothery and J. W. Christian, *Philos. Mag., 36,* 835-842 (1945). (Equi Diagram, Crys Structure; Experimental)

**48And:** K. W. Andrews, *Res., 1,* 478-479 (1948). (Equi Diagram, Crys Structure; Review)

**50Pea:** W. B. Pearson, *J. Iron Steel Inst., 164,* 149-159 (1950). (Equi Diagram; Review; #)

**50Pie:** P. Pietrokowsky and P. Duwez, *Trans. AIME, 188,* 1283-1284 (1950). (Crys Structure; Experimental)

**50Sho:** D. P. Shoemaker and B. G. Bergman, *J. Am. Chem. Soc., 72,* 5793 (1950). (Crys Structure; Experimental)

**51Pea:** W. B. Pearson, J. W. Christian, and W. Hume-Rothery, *Nature, 167,* 110 (1951). (Equi Diagram; Experimental, Review)

**51Sul:** A. H. Sully, *J. Inst. Met., 80,* 173-179 (1951). (Crys Structure; Review; #)

**52Mar:** H. Martens and P. Duwez, *Trans. ASM, 44,* 484-493 (1952). (Equi Diagram, Crys Structure; Experimental)

**52Pea:** W. B. Pearson and J. W. Christian, *Acta Crystallogr., 5,* 157-162 (1952). (Crys Structure; Experimental)

**54Gre:** P. Greenfield and P. A. Beck, *Trans. AIME, 200,* 253-257 (1954). (Equi Diagram, Crys Structure; Experimental)

**54Luc:** W. R. Lucas and W. D. Fishel, *Trans. ASM, 46,* 277-289 (1954). (Equi Diagram; Experimental)

**54Ros:** W. Rostoker and A. Yamamoto, *Trans. ASM, 46,* 1136-1163 (1950). (Equi Diagram, Crys Structure; Experimental)

**55Nev:** M. V. Nevitt and P. A. Beck, *Trans. AIME, 203,* 699-674 (1955). (Equi Diagram; Experimental)

**55Sut:** A. L. Sutton and W. Hume-Rothery, *Philos. Mag., 46,* 1295-1309 (1955). (Equi Diagram, Crys Structure; Experimental)

**56Kas:** J. S. Kasper and R. M. Waterstrat, *Acta Crystallogr., 9,* 289-295 (1956). (Crys Structure; Experimental)

**56Bec:** P. A. Beck, J. B. Darby, and O. P. Arora, *Trans. AIME, 206,* 148-149 (1956). (Meta Phases; Experimental)

**57Hel:** A. Hellawell and W. Hume-Rothery, *Philos. Trans. Roy. Soc. London, A249,* 417-459 (1957). (Equi Diagram; Experimental)

**57Phi:** T. V. Philip and P. A. Beck, *Trans. AIME, 209,* 1269-1271 (1957). (Meta Phases; Experimental)

**57Zak:** M. I. Zakharova and P. N. Stetsenko, *Vestn. Mosk. Univ., Ser. Mat. Mekh. Astron., Fiz. Khim., 11,* 53-61 (1957). (Meta Phases; Experimental)

**58Zak:** M. I. Zakharova, I. A. Ignatova, L. A. Semenova, and N. A. Khatanova, *Dokl. Akad. Nauk SSSR, 119,* 498-500 (1958); TR: *Proc. Acad. Sci. USSR, Chem. Sect., 119,* 227-229 (1958). (Meta Phases; Experimental)

**59Bun:** K. Bungardt and W. Spyra, *Arch. Eisenhüttenwes., 30,*

95-102 (1959). (Equi Diagram; Experimental)
**59Dwi:** A. E. Dwight, *Trans. AIME, 215,* 283-286 (1959). (Crys Structure; Experimental)
**59Stu:** H. P. Stüwe, *Trans. Met. Soc. AIME, 215,* 408-411 (1959). (Crys Structure; Review)
**59Zak:** M. I. Zakharova, L. A. Semenova, and P. N. Stetsenko, *Izv. Akad. Nauk SSR, Otd. Tekhn. Nauk, Met. Topl.,* (5), 135-138 (1959). (Meta Phases; Experimental)
**60Che:** C. H. Cheng, C. T. Wei, and P. A. Beck, *Phys. Rev., 120,* 426-436 (1960). (Equi Diagram, Thermo; Experimental)
**60Lis:** A. G. Lisnik and V. P. Skvorchuk, *Dop. Akad. Nauk Ukr. RSR,* (10). 1408-1412 (1960). (Equi Diagram; Experimental)
**60Par:** D. Parsons, *Nature, 185,* 839-840 (1960). (Equi Diagram; Experimental)
**61Sch:** K. Schröder, *J. Appl. Phys., 32,* 880-882 (1961). (Thermo; Theory)
**61Wei:** C. T. Wei, C. H. Cheng, and P. A. Beck, *Phys. Rev., 122,* 1129-1130 (1961). (Thermo; Experimental)
**52Ara:** S. Arajs, R. V. Colvin, H. Chessin, and J. M. Peck, *J. Appl. Phys., 33,* 1353-1354 (1962). (Equi Diagram; Experimental)
**62Cha:** R. J. Chandross and D. P. Shoemaker, *J. Phys. Soc. Jpn., 17, Suppl. B-III,* 16-19 (1962). (Crys Structure; Experimental)
**62Mat:** P. M. Matveeva, *Akad. Nauk SSSR* (1955), cited by A. E. Vol in *Constitution and Properties of Binary Metallic Systems,* Vol. II, Gosudarst. Izdatel., Moscow, 9-20 (1962). (Equi Diagram; Review)
**62Sax:** R. K. Saxer, Ph.D. thesis, Ohio State Univ. (1962). (Thermo; Experimental)
**63Che:** H. Chessin, S. Arajs, and D. S. Miller, *Adv. X-Ray Anal., 6,* 121-135 (1963). (Crys Structure; Experimental)
**63Kau:** L. Kaufman, E. V. Clougherty, and R. J. Weiss, *Acta Metall. 11,* 323-335 (1963). (Thermo; Theory)
**63Nev:** M. V. Nevitt and A. T. Aldred, *J. Appl. Phys., 34,* 463-468 (1963). (Equi Diagram; Experimental)
**63Scu:** R. G. Scurlock and E. M. Wray, *Phys. Lett., 6,* 28-29 (1963). (Thermo; Experimental)
**64Bre:** D. F. Brewer, D. R. Howe, and B. G. Turrell, *Phys. Lett.,* 13, 204-205 (1964). (Thermo; Experimental)
**64Dai:** M. Daire, *Compt. Rend., 259,* 2640-2642 (1964). (Meta Phases; Experimental)
***64Han:** R. E. Hanneman and A. N. Mariano, *Trans. AIME, 230,* 937-939 (1964). (Equi Diagram, Crys Structure, Thermo; Experimental)
**64Lor:** T. R. Loree, *Bull. Am. Phys. Soc., 9,* 534 (1964). (Equi Diagram; Experimental)
**64Myl:** K. M. Myles and A. T. Aldred, *J. Phys. Chem., 68,* 64-69 (1974). (Thermo; Experimental)
***65Han:** R. E. Hanneman, R. E. Ogilvie, and H. C. Gatos, *Trans. Met. Soc. AIME, 233,* 685-691, 691-698 (1965). (Equi Diagram, Thermo; Experimental; #)
**65Rap:** R. L. Rapson, Thesis, Air Force Inst. of Tech., WPAFB, Ohio School of Engr. Rep. GEM/ME/65-1, quoted in [Hultgren II]. (Thermo; Experimental)
**66Nit:** L. P. Nitikin, A. V. Kogan, V. D. Kul'dov, and I. P. Shiryapov, *Sov. Phys. JETP, 22,* 714-716 (1966); *Zh. Eksp. Teor. Fiz., 49,* 1028-1030 (1965). (Thermo; Experimental)
**67Sch:** K. Schröder and M. Yessik, *J. Phys. Chem. Solids,* 28, 291-295 (1967). (Thermo; Experimental)
**68Hah:** A. Hahn and E. P. Wohlfarth, *Helv. Phys. Acta, 41,* 857-868 (1968). (Equi Diagram; Theory)
***70Fis:** W. A. Fischer, K. Lorenz, H. Fabritius, and D. Schlegel, *Arch. Eisenhüttenwes., 41,* 489-498 (1970). (Equi Diagram; Experimental)
**70Fru:** R. J. Fruehan, *Met. Trans., 1,* 2083-2088 (1970). (Thermo; Experimental)
**70Kir:** G. Kirchner and G. Gemmel, quoted in [83And]. (Equi Diagram; Experimental)
**70Kau:** L. Kaufman and H. Bernstein, *Computer Calculation of Phase Diagrams,* Academic Press, New York, 184 (1970). (Thermo; Theory)
**71Wei:** C. W. Weidner, Jr., Ph.D. thesis, Ohio State Univ. (1971). (Thermo; Experimental)
**72Ald:** A. T. Aldred, *Int. J. Magn., 2,* 223-230 (1972). (Equi Diagram; Experimental)
**73Kov1:** K. Kovacova and F. Kralik, *Kovove Mater., 11,* 93-97 (1973). (Equi Diagram; Experimental)
**73Kov2:** K. Kovacova, *Kovove Mater., 11,* 197-202 (1973). (Thermo; Theory)
**73Mal:** I. Malinsky and F. Claisse, *J. Chem. Thermodyn., 5,* 911-916 (1973). (Thermo; Experimental)
**73Ore:** J. Orehotsky and K. Schröder, *Phys. Status Solidi (a), 19,* 93-102 (1973). (Thermo; Experimental)
***73Spe:** P. J. Spencer and F. H. Putland, *J. Iron Steel Inst., 211,* 293-297 (1973). (Equi Diagram, Thermo; Experimental, Theory; #)
**75Cla:** H. Claus, *Phys. Rev. Lett., 34,* 26-29 (1975). (Equi Diagram; Experimental)
**75Dyu:** V. G. Dyubanov, A. Ya. Stomakhin, and A. F. Filippov, *Izv. V.U.Z. Chernaya Metall.,* (3), 5-7 (1975). (Thermo; Experimental)
**75Fur:** T. Furukawa and E. Kato, *Tetsu-to-Hagané, 61,* 3050-3059 (1975). (Equi Diagram, Thermo; Experimental)
**76Nor:** A. S. Normanton and B. B. Argent, *Met. Sci., 10,* 243-248 (1976). (Thermo; Experimental)
**76Rob:** D. Robinson and B. B. Argent, *Met. Sci., 10,* 219-221 (1976). (Thermo; Experimental)
***77Kub:** O. Kubaschewski, H. Probst, and K. H. Geiger, *Z. Phys. Chem. Neue Folge, 104,* 23-30 (1977). (Equi Diagram, Thermo; Experimental; #)
**78Myd:** J. A. Mydoch, *J. Magn. Magn. Mater., 7,* 237-248 (1978). (Equi Diagram; Theory)
**78Sed:** V. D. Sedykh, *Acta Crystallogr., A34, Suppl. 1.5-4, S14* (1978). (Crys Structure; Experimental)
**79Ber:** C. Bernard, Domaine University, Grenoble, France, private communication quoted in [79Hac]. (Equi Diagram; Theory)
**79Bok:** B. S. Bokshtein and E. B. Guglya, *Izv. V.U.Z. Chernaya Metall.,* (5), 98-100 (1979); *Chem. Abs. 91:94995.* (Crys Structure; Experimental)
**79Chi:** M. Chiriac and G. Inden, unpublished results quoted in [79Hac], [79Spe], and [81Gal]. (Equi Diagram; Experimental)
***79Hac:** K. Hack, H. D. Nüssler, P. J. Spencer, and G. Inden, *Calphad VIII,* Royal Inst. of Tech., Stockholm, 244-265 (1979). (Equi Diagram, Thermo; Theory; #)
**79Hay:** F. H. Hayes and R. Kubitz, *Calphad VIII,* Royal Inst. of Tech., Stockholm, 229-243 (1979). (Thermo; Theory)
**79Ohl:** D. Ohlendorf, E. Wicke, and A. Obermann, *J. Phys. Chem. Solids, 40,* 849-856 (1979). (Thermo; Experimental)
**79Spe:** P. J. Spencer, in *Calculation of Phase Diagrams and Thermochemistry of Alloy Phases,* Y. A. Chang and J. F. Smith, Ed., TMS-AIME, Warrendale, PA, 14-25 (1979). (Thermo; Theory)
**81Bat:** G. I. Batalin, V. S. Sudavtsova, and Yu. K. Vysotskii, *Ukr. Khim. Zh., 47*(10), 1093-1094 (1981). (Thermo; Experimental)
**81Gal:** R. Gallagher, H. D. Nüssler, and P. J. Spencer, *Physica, 103B,* 8-20 (1981); Proc. Int. Symp. Thermo. Alloys, Delft 12-13 Jun 1980. (Equi Diagram; Theory)
**81Ily:** N. G. Ilyushchenko, N. I. Shurov, and E. G. Kazanskii, *Zh. Fiz. Khim., 55,* 2692-2693 (1981); *Russ. J. Phys. Chem., 55,* 1531-1532 (1981). (Thermo; Experimental, Theory)
**81Smi:** J. F. Smith, *Bull. Alloy Phase Diagrams, 2*(1), 40-41; *2*(2) 172 (1981). (Equi Diagram; Review; #)
**82Bal:** Yu. V. Balkovoi, R. A. Aleev, and V. A. Grigoryan, *Izv. V.U.Z. Chernaya Metall.,* (3), 151 (1982); *Chem. Abs. 97:116224h.* (Thermo; Experimental)
**82Bat:** G. I. Batalin, V. S. Sudavtsova, and Yu. K. Vysotskii, *Izv. Akad. Nauk SSSR, Met.,* (6), 52-54 (1982); *Ukr. Khim. Zh., 47*(10), 1093-1094 (1981). (Thermo; Experimental)
**82Igu:** Y. Iguchi, S. Nobori, K. Saito, and T. Fuwa, *Tetsu-to-Hagané, 68,* 633-640 (1982). (Thermo; Experimental)
***82Kub:** O. Kubaschewski, *Iron—Binary Phase Diagrams,* Springer-Verlag, Berlin, 160-164 (1982). (Equi Diagram; Review; #)
**82Mir1:** I. Mirebeau and G. Parette, *J. Appl. Phys., 53,* 1960-1962 (1982). (Equi Diagram; Experimental)
**82Mir2:** I. Mirebeau, M. C. Cadeville, G. Parette, and I. A. Campbell, *J. Phys. F (Met. Phys.), 12,* 25-37 (1982). (Crys Structure; Experimental)
**82Swa:** L. J. Swartzendruber, *Bull. Alloy Phase Diagrams, 3*(2),

161-165 (1982). (Equi Diagram; Review; #)
***83And:** J. O. Andersson, *Calphad*, 7, 295-305 (1983). (Equi Diagram, Thermo; Theory; #)
***83But:** J. Büth, Ph.D. thesis, Max Planck Inst. für Eisenforsch., Düsseldorf: G. Inden, thesis research advisor (1983). (Equi Diagram, Thermo; Experimental; #)

*Indicates key paper.
#Indicates presence of a phase diagram.

Fe-V evaluation contributed by **J. F. Smith,** Ames Laboratory-USDOE and Department of Materials Science and Engineering, Iowa State University, Ames, Iowa 50011. Work was done at the Ames Laboratory, which is operated for the U.S. Department of Energy, under contract No. W-7405-Eng-82. That portion of the work dealing with assessment of phase relationships and crystallography was supported by the Office of Basic Energy Sciences, Division of Materials Sciences (AK-01-02). That portion of the work dealing with thermodynamic assessment was supported by the Department of Energy through the Joint Program on Critical Compilation of Physical and Chemical Data coordinated through the Office of Standard Reference Data, National Bureau of Standards. Literature searched through 1982. Professor Smith is the ASM/NBS Program Category Editor for binary vanadium alloys.

# The Fe-N-V (Iron-Nitrogen-Vanadium) System

55.847 14.0067 50.9415

**By V. Raghavan**
**Indian Institute of Technology–Delhi**

Most of the published data concern the solubility of N in Fe-rich Fe-V alloys in the liquid state, in austenite, and in ferrite. Only [78Els] presented two isothermal sections covering the entire composition range. The data starting with the work of [78Els] are discussed below in separate sections, including, in each instance, the experimental techniques used.

## Binary Systems

The Fe-rich end of the Fe-N phase diagram has been determined at temperatures below 700 °C and at very high pressures, corresponding to the dissociation of $NH_3$. Three intermediate phases, $\gamma'$, $Fe_4N$, (fcc: 19.4 to 20.6 at.% or 5.7 to 6.1 wt.% N), $\varepsilon$ (cph: 23.9 to 33.2 at.% or 7.3 to 11.1 wt.% N) and $\zeta$, $Fe_2N$, (orthorhombic: 33.2 to 33.7 at.% or 11.1 to 11.3 wt.% N), are known in this range [48Jac]. Two eutectoid reactions occur [79Agr]:

$\varepsilon \rightarrow \gamma + \gamma'$ at 650 °C and 15.97 at.% (4.55 wt.%) N

and

$\gamma \rightarrow \alpha + \gamma'$ at 592 °C and 8.97 at.% (2.41 wt.%) N

Fe-V alloys [84Smi] solidify as a continuous series of solid solutions, with an azeotropic minimum at 1468 °C and 31.0 at.% (29.1 wt.%) V. At lower temperatures, a closed gamma loop forms with the upper limit of the two-phase field at 2.0 at.% (1.83 wt.%) V. An intermediate phase, $\sigma$, centered around the composition FeV, has a congruent formation temperature of 1219 °C.

In the N-V system [49Hah, 64Bra], two compounds ($V_{2-3}N$ and VN) form, with a fairly wide homogeneity range. This phase diagram has not been determined in detail.

## Binary Compounds

In the phase diagrams presented here, the iron nitride phases do not appear. For more details on these, see [48Jac]. The $\sigma$ phase in the Fe-V system is isostructural with the $\sigma$CrFe phase, with 30 atoms in the tetragonal cell (see Table 1). VN has the NaCl cubic structure, often deficient in N. $V_{2-3}N$ has a composition range that extends from the formula $V_3N$ to $V_2N$. It forms the interstitial-type cph structure; lattice parameters are listed in Table 1. Metastable, transition V-N compounds, formed by low-temperature aging of quenched alloys with 0 to 10 at.% N, were reported by [71Hen, 74Pot]. These are not listed in Table 1. No ternary compounds were found by [78Els].

## Isothermal Sections

[78Els] used X-ray methods, metallography, and microprobe analysis to construct the isothermal sections at 1100 and 1200 °C. They reported that their results correspond to a pressure of $\sim 10^{-9}$ MPa of $N_2$. Under such low pressures, the V-N compounds shown in their isothermal sections are expected to dissociate [64Bra]. Some contamination by oxygen was also reported by [78Els]. In view of these and the absence of corroborative data by others, the results of [78Els] may be considered tentative. Figure 1 shows their isothermal section at 1100 °C, redrawn to agree with the Fe-V binary data of [84Smi]. The inset shows schematically the nominal solubility along the binary axes. The congruent formation temperature of the $\sigma$ phase was given as 1135 ± 20 °C by [78Els]. The value from the accepted Fe-V binary diagram [84Smi] is considerably higher, 1219 °C. Thus, the $\sigma$ phase should appear also in the isothermal section at 1200 °C, even though this section presented by [78Els] does not show the $\sigma$ phase. [78Els] also reported a eutectic reaction in the quasibinary Fe-VN section at 1500 ± 20 °C at 1 bar of $N_2$ pressure.

## Solubility of N in Liquid Alloys

The solubility of N in liquid Fe-V alloys was determined by the Sieverts' method [29Sie] by [58Kas, 60Peh, 61Rao, 62Kor1, 63Kor, 63Tay, 65Eva, 81Sch, 81Wad]. An inherent error here is the vaporization and the subsequent condensation of the metal in the reaction chamber. This error was minimized by [60Peh, 63Tay] by avoiding low total pressures over the melt through partial evacuation of the insoluble gas in the reaction chamber and by using the minimum time required for equilibrium. The approach to equilibrium was checked by [58Kas, 60Peh, 63Tay, 81Wad] from both directions by raising or lowering pressure (or temperature). In the sampling method, the melt is allowed to reach equilibrium with the gas and then a sample is withdrawn, quenched, and analyzed for N [40Bri, 60Mae, 82Ish]. Levitation melting followed